Micromagnetic simulation of magnetization reversal processes in ferromagnetic cubes from quasisaturation state

2002 J. Phys.: Condens. Matter 14 8089

(http://iopscience.iop.org/0953-8984/14/34/327)

INSTITUTE OF PHYSICS PUBLISHING JOURNAL OF PHYSICS: CONDENSED MATTER

J. Phys.: Condens. Matter **14** (2002) 8089–8101 PII: S0953-8984(02)35862-4

Micromagnetic simulation of magnetization reversal processes in ferromagnetic cubes from quasisaturation state

Mai Lu[1] **and Paul J Leonard**

Department of Electronic and Electrical Engineering, University of Bath, Claverton Down, Bath BA2 7AY, UK

E-mail: eesml@bath.ac.uk

Received 15 April 2002
Published 15 August 2002
Online at stacks.iop.org/JPhysCM/14/8089

Abstract

Recent divergence in analysing the magnetization processes in isolated particles between analytical micromagnetics and numerical micromagnetics has focused on whether it is necessary to use nucleation theory in the analysis. Complete saturation is the necessary condition for using nucleation theory. A ferromagnetic elliptical particle can be uniformly magnetized in a large field. As the field decreases, there exists a nucleation field at which the magnetization deviates from uniform magnetization. On the contrary, a ferromagnetic cube can never be saturatedly magnetized in any finite homogeneous field. It is difficult to apply the theory of a nucleation field of an elliptical particle to a cubic particle. One practical way to discuss the 'nucleation' in a cubic particle is to supervise the magnetization changes from a positive quasisaturation state to a negative quasisaturation state, and find what kind of reversal modes appear. In this paper, a three-dimensional micromagnetics model is implemented to analyse the magnetization reversal processes in cubic particles at a field (1.1×10^6 Oe) where the quasisaturation is well developed in a cubic particle. The sizes of particles vary from 400–1000 Å. A fine mesh with $10 \times 10 \times 10$ and a small decreasing step of applied field 10 Oe are used in the calculations. The 'nucleation' in a cubic particle starts from the quasiquantization state (flower state). For a particle whose size is smaller than 1000 Å, the equilibrium magnetization states during magnetization reversal processes are a flower state and an anti-flower state, and a coherent rotation happens when the magnetization state changes from a flower state to an anti-flower state. For a larger particle with a size of 1000 Å, there exist rather complicated equilibrium magnetization states i.e. a flower state, anticlockwise vortex state, intermediate state, clockwise vortex state, and anti-flower state all appear during the reversal processes.

[1] Author to whom any correspondence should be addressed.

0953-8984/02/348089+13$30.00

1. Introduction

The theory of micromagnetics using a continuous magnetization vector began with the wall calculation of Landau and Lifshitz [1]. The origin and principles of the theory were reviewed and discussed by Brown [2, 3], in which the atomic structure of matter is ignored. Early applications of micromagnetic modelling on isolated particles were in the area of elliptically shaped particles, which used the linear Brown equations, and discussed the nucleation problem. Generally, it is called analytical micromagnetics or classical micromagnetics [4].

It is well known that an elliptical particle can be saturatedly magnetized along its major axis because the demagnetizing field in it is homogeneous, and this complete saturation is the necessary condition for using nucleation theory, i.e. an elliptical particle is put into a magnetic field which is large enough to saturate it. Then the field is reduced slowly. At some point, the state of saturation along the original direction of the applied field stops being stable, and some changes start to take place. This field is called the nucleation field, and the corresponding magnetization distribution is called the nucleation mode or magnetization reversal mode. Usually they are the coherent rotation mode, curling mode, or buckling mode.

In the middle of the 1960s, Brown started to solve the micromagnetics problem (one-dimensional domain wall) by computer simulation [5], and this method was developed by Labonte to solve two-dimensional Bloch-type domain walls [6]. In these calculations, four kinds of energy (exchange energy, crystalline energy, demagnetizing energy and Zeeman energy) are considered and the minimization of the total free energy is achieved by rotating the magnetization vector in each mesh element to the effective field with the aid of the computer, and yields both the hysteresis loops and the magnetization distributions. Compared with the classical micromagnetics, the calculation of magnetization problems in magnetic materials in the above two papers start from the minimization of free energy by computer, not from the Brown equations. Usually we call this numerical micromagnetics.

Numerical micromagnetics has developed very rapidly over the past decade as high performance computers became available. Numerical micromagnetics is especially suited for solving thin film problems, but meets some opposite opinions in dealing with ferromagnetic nonelliptical fine particles. The main divergence between analytical micromagnetics and numerical micromagnetics is in focusing on whether it is necessary for us to use nucleation theory in numerical micromagnetics, especially in the calculation of nonelliptical particles, such as prisms [7–9]. As discussed above, there are two premises in using nucleation theory:

(i) the demagnetizing field is homogeneous in a particle,
(ii) the particle is saturatedly magnetized.

Since a cubic particle cannot be saturated in any finite, homogeneous magnetic field, and its demagnetizing field is also inhomogeneous, most research ignored nucleation theory in this kind of calculation, and the starting point of calculations of the magnetization reversal process was selected randomly (usually a relatively small applied field is used in these calculations). So the results in these papers were questioned by some theorists.

In this paper, we re-calculate the magnetization processes in cubic particles by using Aharoni's suggestion [9], i.e. computations start at a field where the quasisaturation is well developed in a cubic particle, which is not very different from the requirement for starting computations for an ellipsoid from a completely saturated state. But one thing should be emphasized no matter how large the applied field is: the 'nucleation' in a cubic particle starts from a state in which the magnetization changes continuously with the changing applied field. So we cannot get a distinct nucleation field as in an elliptical particle. But we can supervise and record the changes of the magnetization distributions during the magnetization reversal processes and find what kind of reversal modes appear during the reversal processes.

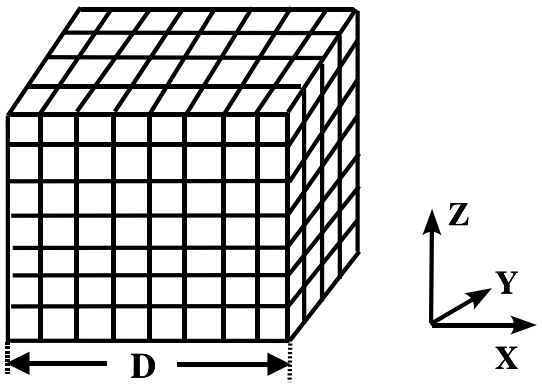

Figure 1. A cubic particle and its discretization procedure. D is the particle size.

Figure 1 shows a cubic particle and its discretization procedure. D labels the particle size. The easy crystalline axis of the particle is assumed to be along the z direction. The material parameters in this paper are the same as those of the earlier paper [10]. The particles are assumed to have uniaxial crystalline anisotropy with an anisotropy constant $K_1 = 18\,500$ erg cm^{-3}, a saturation magnetization $M_s = 370$ emu cm^{-3} and an exchange constant of $A = 10^{-6}$ erg cm^{-1}, which gives the exchange length $l_{ex} = \sqrt{A/M_s^2} = 270$ Å in this paper. Recent calculations show the size of the subdivisions should not be larger than the exchange length of the materials [11]. In this paper, seven particles with sizes 400, 550, 600, 700, 800, 900 and 1000 Å are selected in the computations. Compared with the maximum size of a particle, $D = 550$ Å, in [10], we use a particle with maximum size $D = 1000$Å, because the same magnetization reversal processes were found in a particle whose size is smaller than 1000 Å if the computation starts from quasisaturation state. A fine mesh of $10 \times 10 \times 10$ is used in the following calculations.

2. Numerical model

The micromagnetics model of Schabes and Bertram is followed whereby the particles are discretized into cubic elements in which each cell has a uniform magnetization. The total free energy E_{tot} in a cubic particle is the sum of four contributions:

$$E_{tot} = E_{app} + E_{an} + E_{ex} + E_{mag} \tag{1}$$

where E_{app} is the Zeeman energy describing the interaction of the particle magnetization with an applied field, E_{an} is the magnetocrystalline anisotropy energy, E_{ex} is the exchange energy and E_{mag} is the magnetostatic interaction energy. Writing the magnetization vector as $\vec{M} = M_s(\alpha\vec{i} + \beta\vec{j} + \gamma\vec{k})$ and the applied field as $\vec{H}_{app}$, the Zeeman energy is given as

$$E_{app} = -M_s \int_v (\alpha\vec{i} + \beta\vec{j} + \gamma\vec{k}) \cdot \vec{H}_{app}\, \mathrm{d}v \tag{2}$$

where v indicates integration over the volume of the particle, the applied field and the magnetization can be spatially varying. α, β and γ are directional cosines of the magnetization.

The crystalline anisotropy is treated phenomenologically by writing

$$E_{an} = \int_v W_u\, \mathrm{d}v \tag{3}$$

where W_u is an expression of the local crystalline energy density in terms of the directional cosines of the magnetization. For the uniaxial case with easy axis along the z direction, $W_u = K_1 \sin^2\theta$, K_1 is the anisotropy constant and θ is the angle between the z direction and the direction of the magnetization.

The exchange interaction is a quantum mechanical effect and the exchange energy is given by

$$E_{ex} = \int_v A[(\nabla\alpha)^2 + (\nabla\beta)^2 + (\nabla\gamma)^2]\,\mathrm{d}v \tag{4}$$

where A is the exchange constant.

The magnetostatic interaction energy may be written as

$$E_{mag} = -\tfrac{1}{2}\int_v \vec{H}_d \cdot \vec{M}\,\mathrm{d}v \tag{5}$$

where $\vec{H}_d$ is the demagnetizing field from $\vec{H}_d = -\nabla U$ and can be calculated from magnetostatic volume and surface charges.

The equilibrium state of a particle during magnetization reversal processes at a specific applied field corresponds to a minimum of the free energy, expressed by the vanishing at all points of the torques $\vec{T} = \vec{M} \times \vec{H}_{eff}$ exerted on the magnetization in each element, where $\vec{H}_{eff}$ is the effective field, which is defined as

$$\vec{H}_{eff} = -\partial E_{tot}/\partial\vec{M} \tag{6}$$

and can be written as

$$\vec{H}_{eff} = \vec{H}_{app} + \vec{H}_k/M_s(\vec{k}\cdot\vec{M})\vec{k} + 2A/M_s^2\nabla^2\vec{M} + \sum_j N\cdot\vec{M}_j \tag{7}$$

where $\vec{H}_{app}$ is the applied field, $H_k = 2K_1/M_s$ is the uniaxial magnetocrystalline anisotropy field and N is the demagnetizing field tensor. The magnetostatic field involves a sum over all pairwise interactions.

The method for energy minimization is the same as that of Brown and LaBonte's schemes [5, 6]. The magnetization vector in each subdivision is rotated in the direction of $\vec{H}_{eff}$ at that position, after sweeping through all the subdivisions. The maximum angle of this rotation in any of the subdivisions is compared with a preset tolerance ϵ_1. The process of rotating the set of magnetization vectors point by point throughout the grid is continued until this maximum angle is small than the required tolerance. Equilibrium is denoted by the magnetization in each subdivision aligning with the effective field at every point. In this paper $\epsilon = 10^{-4}$ is selected in the calculations.

3. Results and discussions

In theory, if a cubic particle can be magnetized into a saturation state along the z direction, the normalized magnetization vector $\vec{m} = \vec{M}/M_s$ in each subdivision has the relationship $\epsilon_2 = |\vec{m}(i, j, k) - \vec{k}| = 0$, where $\vec{k}$ is the unit vector in the z direction. In practical calculations, different tolerances $\epsilon_2 = 10^{-1}, 10^{-2}, 10^{-3}, 10^{-4}$ are used to find different maximum values of the applied fields. In order to keep the cubic particles quasisaturatedly magnetized, as well as to save computation time, $\epsilon_2 = 10^{-3}$ is selected and the corresponding maximum value of the applied field $H_{app} = 1.1 \times 10^6$ Oe is used in the following calculations.

As mentioned above, the magnetization states will change with the changing applied field in a cubic particle if it is quasisaturatedly magnetized. So the calculations were supervised

for each particle during the magnetization reversal processes from $H_{app} = 1.1 \times 10^6$ to -1.1×10^6 Oe, and the magnetization distributions at some points are recorded.

Figure 2 shows the 2D magnetization distributions for $D = 400$ Å in different layers along the z direction at a remanant state. The vector in each mesh element represents the projection of magnetization in the corresponding subdivision onto the xy plane. A long arrow in a subdivision means the magnetization in this element tilts more towards the xy plane. From figure 2, we know that the angles between a magnetization and the z direction decrease from the first layer to the fifth layer, and then increase from the fifth layer to the tenth layer. This process is similar to the opening process of a flower, and is thus called a flower state in [6], and has been widely adopted in recent micromagnetic simulations to describe the equilibrium magnetization state in nonelliptical particles. We have checked the cubic particle has a flower equilibrium magnetization state even if it is quasisaturatedly magnetized in a large applied field, and this flower state remains in the particle as the applied field decreases from 1.1×10^6 to -1730 Oe, where the magnetizations in all subdivisions start coherent rotation from the positive magnetization direction to the negative magnetization direction. The typical 2D and 3D magnetization distributions of the first and tenth layers at $H_{app} = -1730$ and -1740 Oe are shown in figure 3. The direction of arrows in the 3D figures are parallel to the z direction which is in a direction out of the paper for $H_{app} = -1730$ Oe and into the paper for $H_{app} = -1740$ Oe. A blank square in the 3D figures represents an arrow which points into the paper, and we see the bottom of the arrow. From figure 3, we can conclude: (1) a coherent rotation takes place in the particle as the applied field increases from -1730 to -1740 Oe, and (2) the magnetization distributions in the particle keep the flower states at -1730 and -1740 Oe, but have different characteristics: the flower state closes at the first layer and opens at the tenth layer at $H_{app} = -1730$ Oe (starting point of coherent rotation). After coherent rotation, the flower state opens in the first layer and closes in the tenth layer at $H_{app} = -1740$ Oe (ending point of coherent rotation). Here we define them as a flower state and an anti-flower state, respectively. As the applied field increases in the negative direction further from $H_{app} = -1740$ Oe, the particle will keep the anti-flower state until it is quasisaturatedly magnetized in the negative direction again. As a typical case, figure 4 shows the magnetization distributions of the anti-flower state in different layers along the z direction at $H_{app} = -2000$ Oe. We should emphasize that the coercivity field $Hc = 1735$ Oe for a particle with size $D = 400$ Å obtained in this paper is much larger than that in [10], which started the calculation from a relatively small applied field.

Figures 5 and 6 show the magnetization distributions in a particle with size $D = 550$ Å. The particle keeps a flower state from $H_{app} = 1.1 \times 10^6$ to -880 Oe. Then a coherent rotation takes place and the particle enters into an anti-flower state from $H_{app} = -890$ Oe and keeps this state till $H_{app} = -1.1 \times 10^6$ Oe. Compared with the result of $D = 400$ Å, the flower state and the anti-flower state are more obvious at the starting and ending points of the coherent rotation. The coercivity field $H_c = 885$ Oe in this paper is also much larger than that in [10], which is no larger than 100 Oe, and no vortex magnetization state is found in this paper during magnetization reversal processes from a positive quasisaturation state to a negative quasisaturation state. While in [10], the vortex state appears at a remanant state.

Our calculations show that the pattern of magnetization equilibrium configurations, i.e. flower state $\rightarrow$ coherent rotation $\rightarrow$ anti-flower state, remains in a particle during the magnetization reversal processes if the particle size is smaller than 1000 Å. The calculation results for particles with $D = 600$, 700, 800 and 900 Å are the same as those for $D = 400$ and 550 Å and are omitted here.

Figures 7 and 8 show the equilibrium magnetization distributions in a particle in the bottom layer (first layer) and the top layer (tenth layer) along the z direction at different applied fields

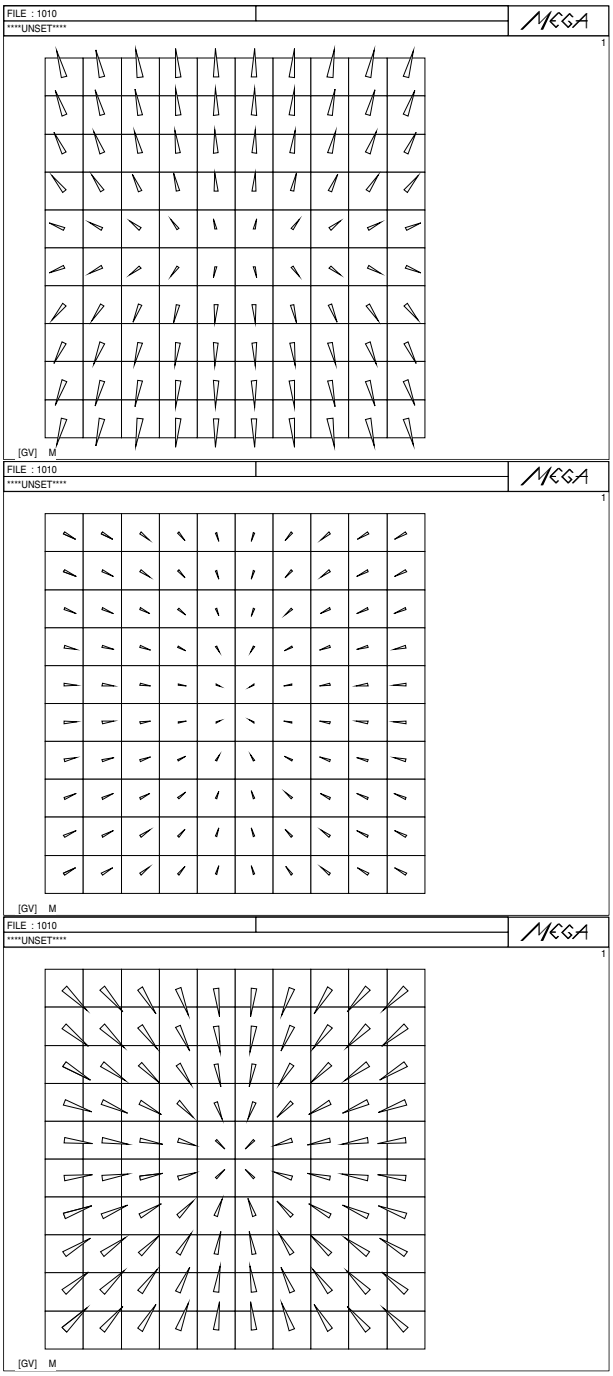

Figure 2. The 2D magnetization distribution for $D = 400$ Å in different layers along the z direction at a remanant state.

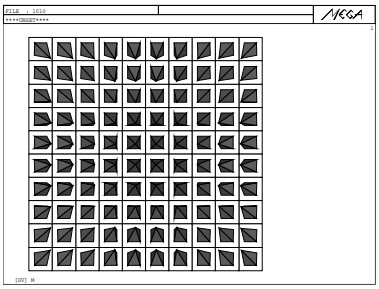

3D for 1st layer at Happ=-1730 Oe

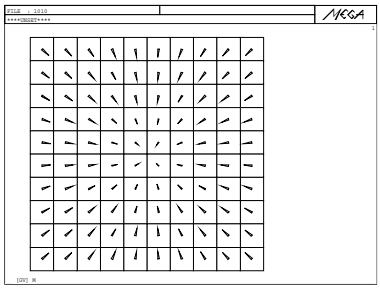

2D for 1st layer at Happ=-1730 Oe

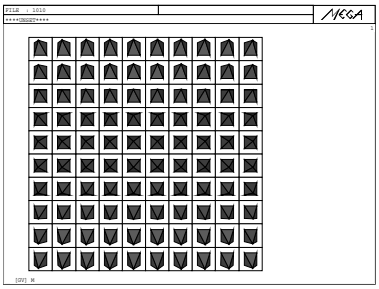

3D for 10th layer at Happ=-1730 Oe

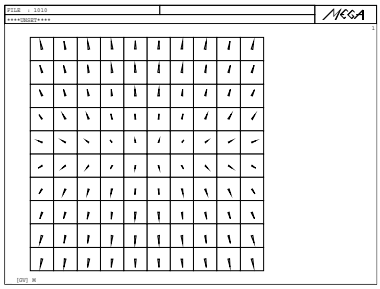

2D for 10th layer at Happ=-1730 Oe

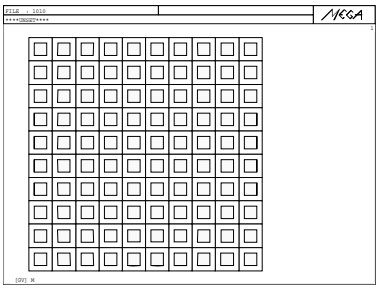

3D for 1st layer at Happ=-1740 Oe

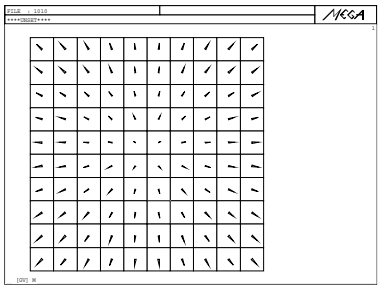

2D for 1st layer at Happ=-1740 Oe

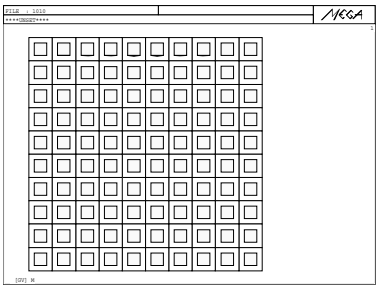

3D for 10th layer at Happ=-1740 Oe

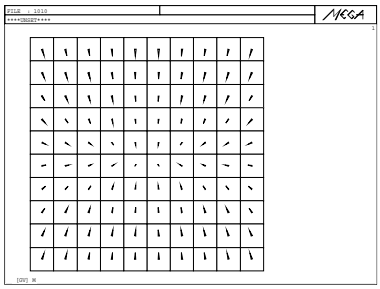

2D for 10th layer at Happ=-1740 Oe

Figure 3. The 2D and 3D magnetization distributions for $D = 400$ Å in the first and tenth layers along the z direction at different applied fields.

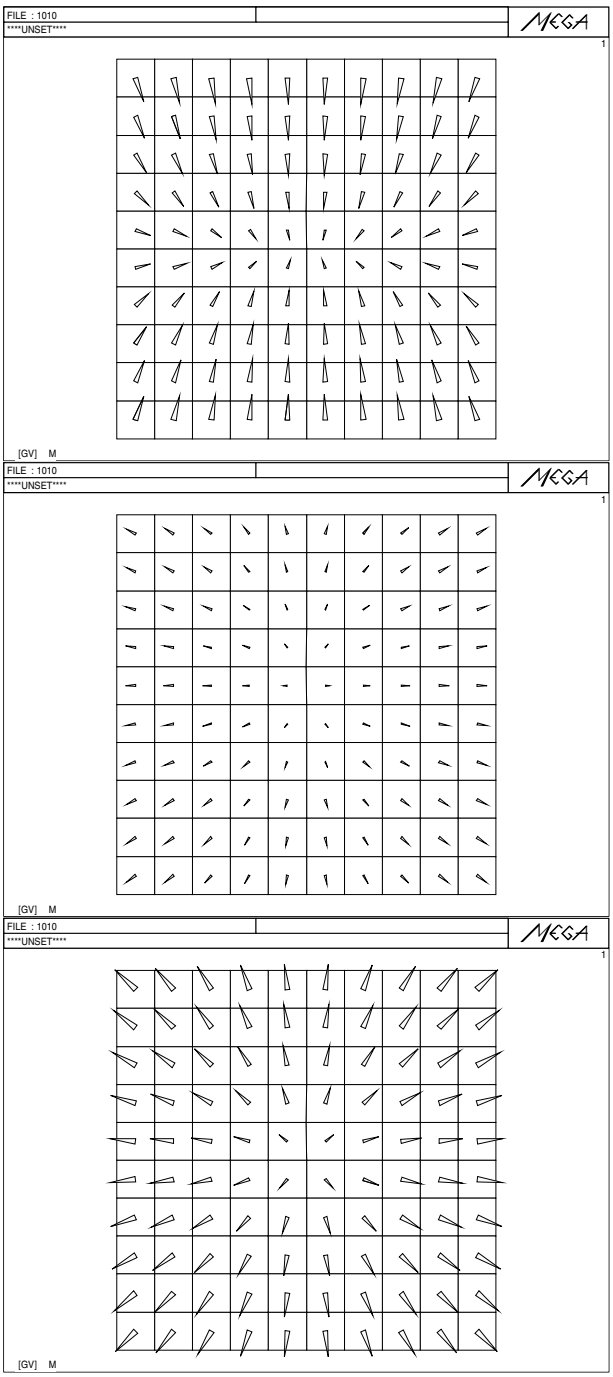

Figure 4. The 2D magnetization distribution for $D = 400$ Å in different layers along the z direction at $H_{app} = -2000$ Oe.

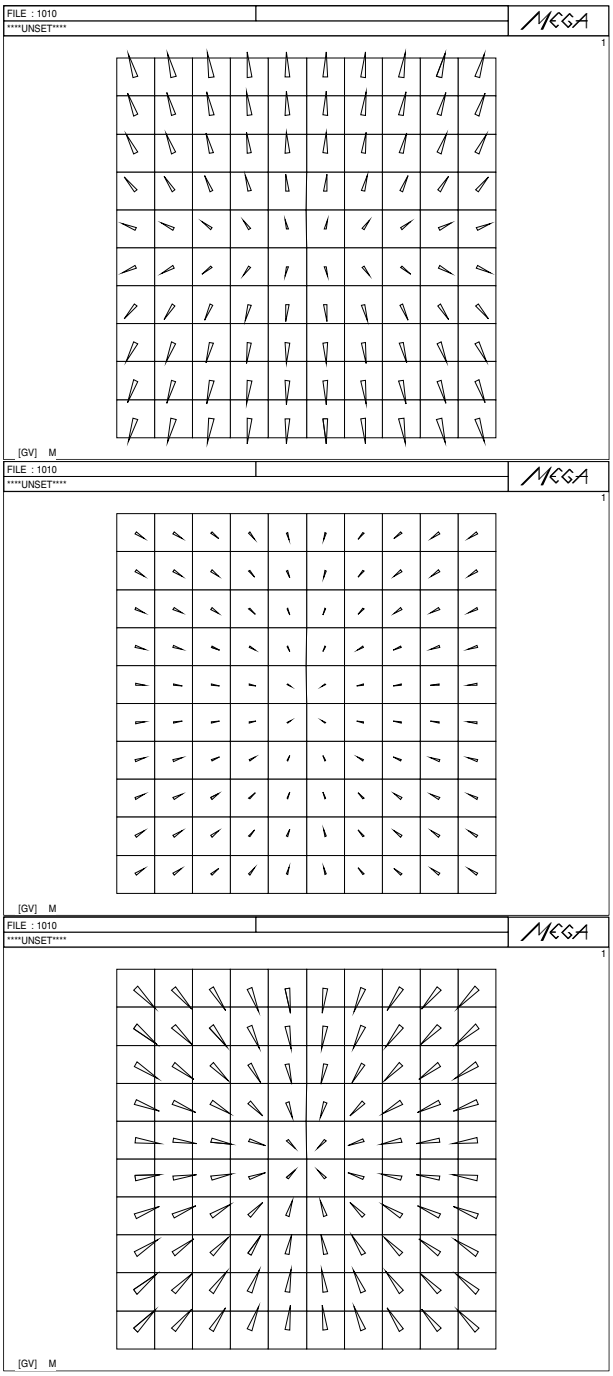

Figure 5. The 2D magnetization distribution for $D = 550$ Å in different layers along the z direction at a remanant state.

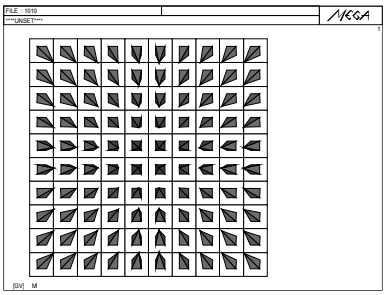

3D for 1st layer at Happ=-880 Oe

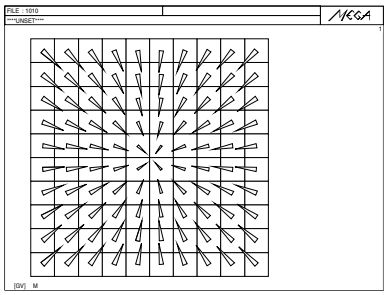

2D for 1st layer at Happ=-880 Oe

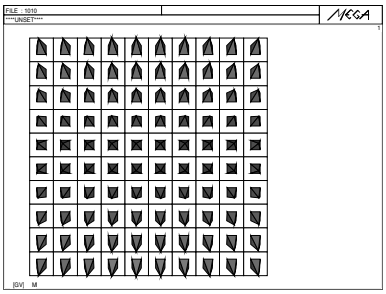

3D for 10th layer at Happ=-880 Oe

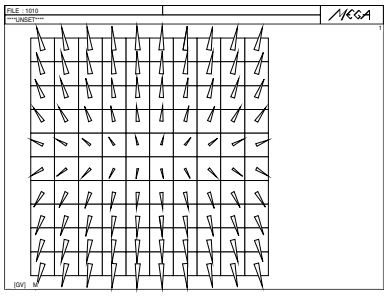

2D for 10th layer at Happ=-880 Oe

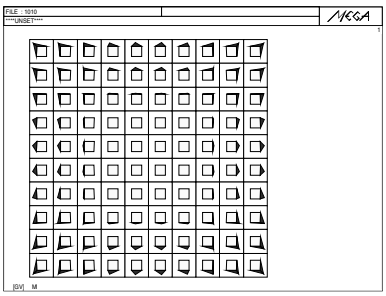

3D for 1st layer at Happ=-890 Oe

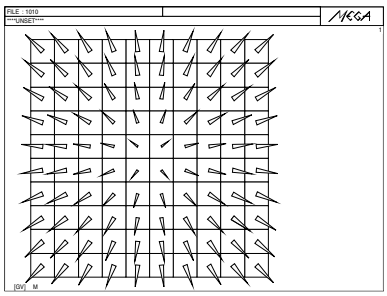

2D for 1st layer at Happ=-890 Oe

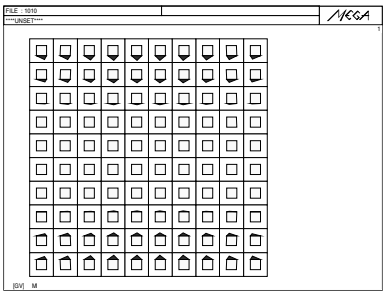

3D for 10th layer at Happ=-890 Oe

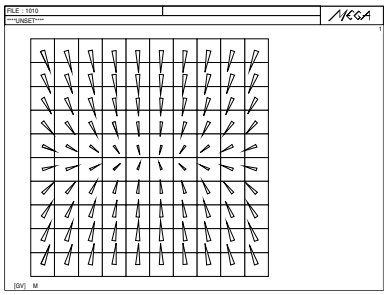

2D for 10th layer at Happ=-890 Oe

Figure 6. The 2D and 3D magnetization distributions for $D = 550$ Å in the first and tenth layers along the z direction at different applied fields.

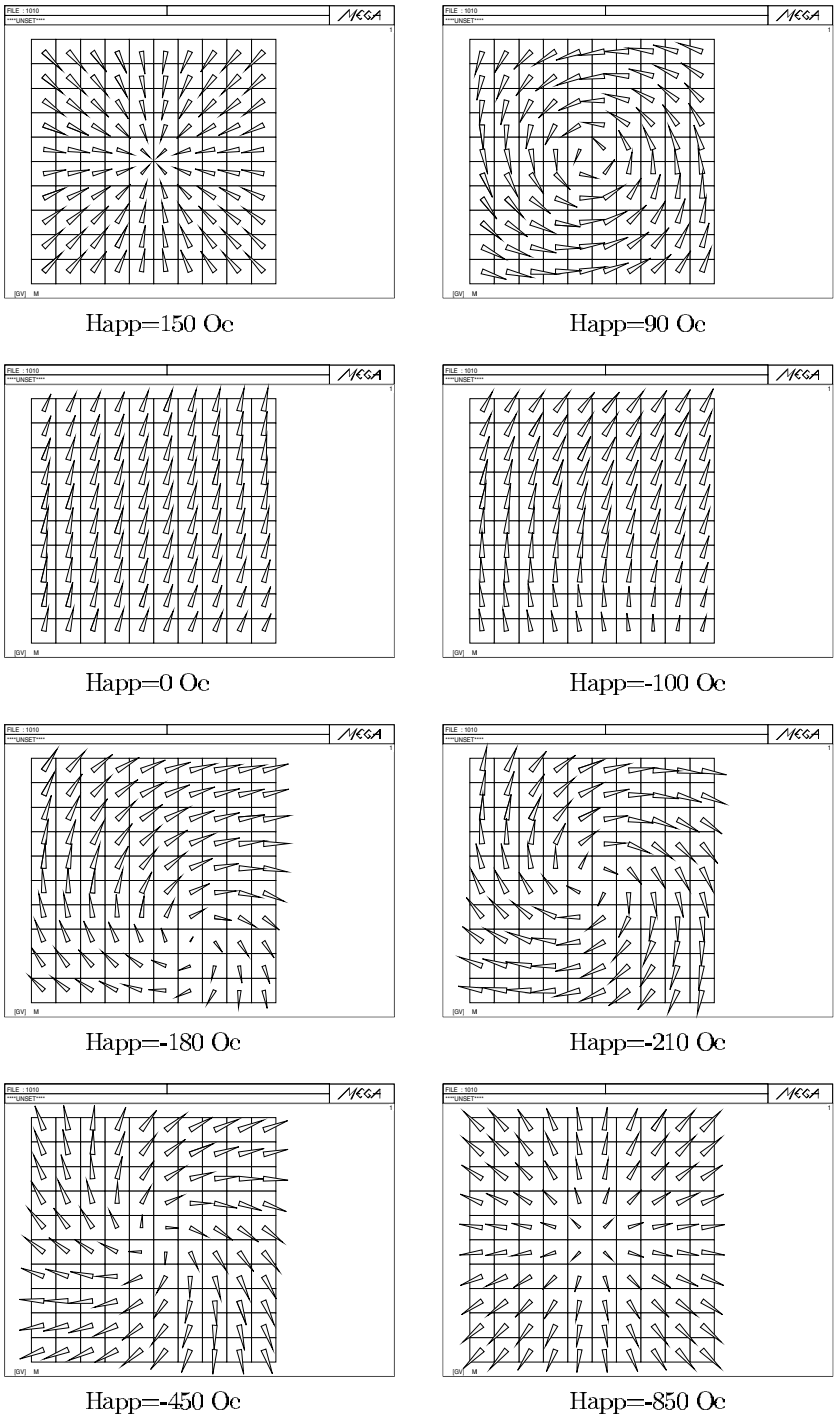

Figure 7. The 2D magnetization distributions for $D = 1000$ Å in the first layer along the z direction at different applied fields.

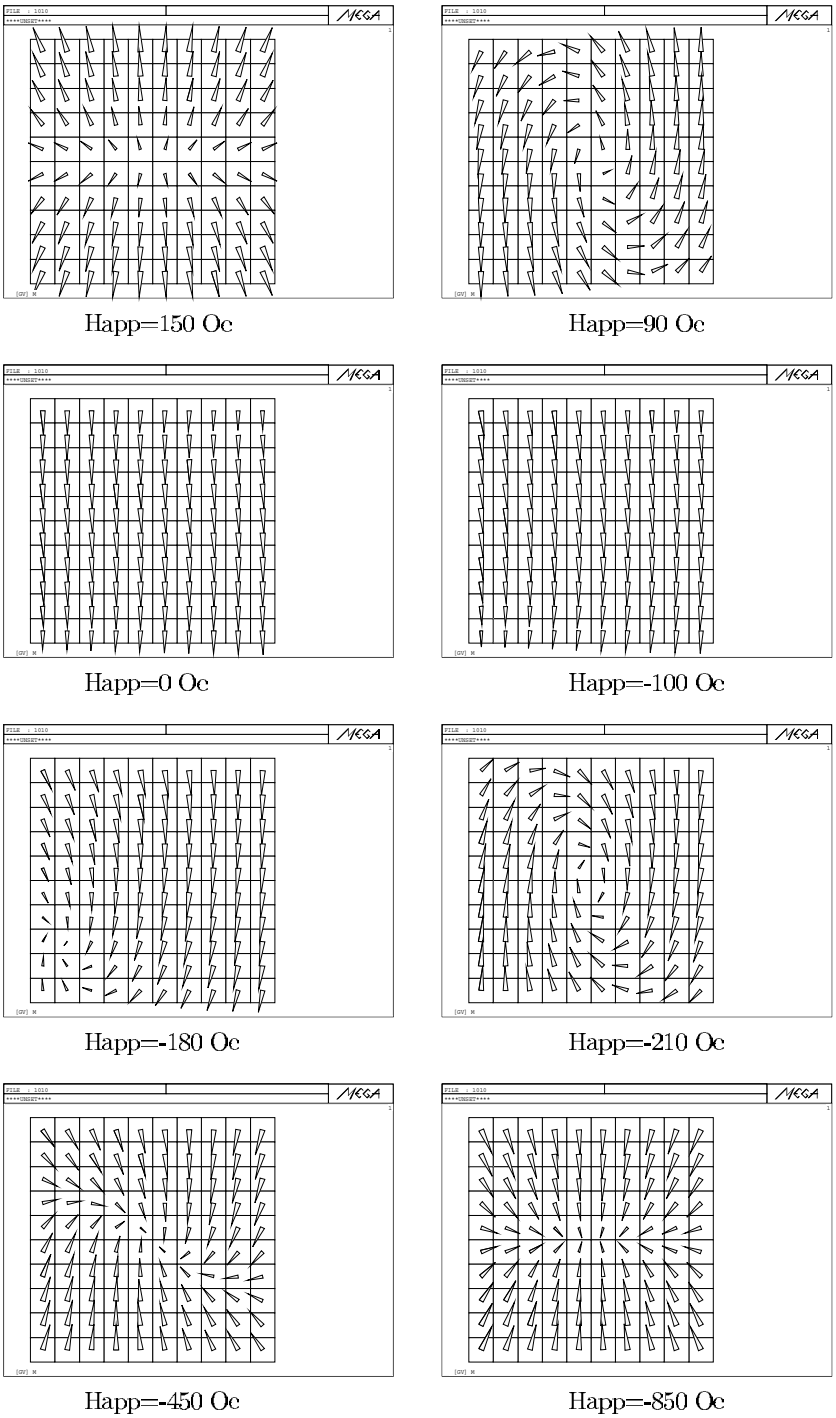

Figure 8. The 2D magnetization distributions for $D = 1000$ Å in the tenth layer along the z direction at different applied fields.

with particle size $D = 1000$ Å. A more complicated magnetization distribution is found in the particle during magnetization reversal processes from a positive quasisaturation state to a negative quasisaturation state. They can be divided into five steps:

(1) From $H_{app} = 1.1 \times 10^6$ to 100 Oe, the equilibrium magnetization distribution is a flower state. A typical figure at $H_{app} = 150$ Oe is shown in figures 7 and 8.
(2) From 90 to 80 Oe, the magnetization distribution suddenly changes from a flower state into an anticlockwise vortex state. A typical figure at $H_{app} = 90$ Oe is shown.
(3) From 70 to -160 Oe, the magnetization distribution is very new, which has not been reported in the previous papers. This state is an intermediate state, which ends the anticlockwise vortex state, and starts a clockwise vortex state. Typical figures at $H_{app} = 0$ Oe (remanant state) and -100 Oe are shown.
(4) From -170 to -750 Oe, the magnetization distribution enters into a clockwise vortex state. Typical figures for $H_{app} = -180$, -210 and -450 Oe are also given.
(5) From -760 to -1.1×10^6 Oe, the clockwise vortex state ends and the particle keeps an anti-flower state until quasisaturatedly magnetized in the negative direction of the applied field. A typical figure for $H_{app} = -850$ Oe is shown in figures 7 and 8.

4. Conclusions

We have calculated the magnetization reversal processes in cubic particles from a quasisaturated state by using a three-dimensional micromagnetics model with a fine mesh and small decreasing steps in the applied field. The equilibrium magnetization states in a cubic particle from positive quasisaturation states to negative quasisaturation states are supervised and recorded. For a particle whose size is smaller than 1000 Å, the pattern of magnetization reversal processes can be simply expressed as: flower state $\rightarrow$ coherent rotation $\rightarrow$ anti-flower state. For a particle with size 1000 Å, this pattern of magnetization reversal processes can be described as: flower state $\rightarrow$ anticlockwise vortex state $\rightarrow$ intermediate state $\rightarrow$ clockwise vortex state $\rightarrow$ anti-flower state. The coercivity fields obtained in this paper are much larger than those in the corresponding literature.

References

[1] Landau L D and Lifshitz E M 1935 *Phys. Z. Sow.* **8** 153
[2] Brown W F Jr 1962 *Magnetostatic Principles in Ferromagnetism* (Amsterdam: North-Holland)
[3] Brown W F Jr 1963 *Micromagnetism* (New York: Wiley–Interscience)
[4] Aharoni A 1996 *Introduction to the Theory of Ferromagnetism* (Oxford: Oxford University Press)
[5] Brown W F Jr and Labonte A E 1965 *J. Appl. Phys.* **36** 1380
[6] Labonte A E 1969 *J. Appl. Phys.* **40** 2450
[7] Aharoni A 1999 *J. Magn. Magn. Mater.* **196–7** 786
[8] Aharoni A 1999 *J. Magn. Magn. Mater.* **203** 33
[9] Aharoni A 1999 *J. Appl. Phys.* **86** 1041
[10] Schabes M E and Bertram H N 1988 *J. Appl. Phys.* **64** 1347
[11] Rave W, Ramstock K and Hubert A 1998 *J. Magn. Magn. Mater.* **183** 329